

# Intermittent thermal convection in jammed emulsions

Francesca Pelusi,<sup>1,\*</sup> Andrea Scagliarini,<sup>1,2</sup> Mauro Sbragaglia,<sup>3</sup> Massimo Bernaschi,<sup>1</sup> and Roberto Benzi<sup>3</sup>

<sup>1</sup>*Istituto per le Applicazioni del Calcolo, CNR - Via dei Taurini 19, 00185 Rome, Italy*

<sup>2</sup>*INFN, Sezione Roma "Tor Vergata", Via della Ricerca Scientifica 1, 00133 Rome, Italy*

<sup>3</sup>*Department of Physics & INFN, University of Rome Tor Vergata,*

*Via della Ricerca Scientifica 1, 00133 Rome, Italy*

(Dated: May 6, 2024)

We study the process of thermal convection in jammed emulsions with a yield-stress rheology. We find that heat transfer occurs via an intermittent mechanism, whereby intense short-lived convective “heat bursts” are spaced out by long-lasting conductive periods. This behaviour is the result of a sequence of fluidization-rigidity transitions, rooted in a non-trivial interplay between emulsion yield-stress rheology and plastic activity, which we characterize via a statistical analysis of the dynamics at the droplet scale. We also show that droplets’ coalescence induced during heat bursts leads to a spatially heterogeneous phase-inversion of the emulsion which eventually supports a sustained convective state.

## I. INTRODUCTION

Concentrated emulsions are binary mixtures of immiscible liquids (say “oil” and “water”), stabilized against phase separation by the presence of surfactants, where droplets of a given phase (e.g., oil) are dispersed in a continuous phase (e.g., water, thus making an oil-in-water, or, in short, O/W, emulsion). When the volume fraction  $\phi$  of the dispersed phase is large enough, droplets are generally strongly deformed, and the emulsion displays a complex non-Newtonian rheology with a non-vanishing yield stress, which is peculiar of materials referred as yield stress materials (YSMs) [1–3]. These materials have been extensively characterized from the rheological point of view. Still, much less is known about their behavior in buoyancy-driven thermal flows, despite their relevance particularly for geophysical problems, such as mantle convection [4–8] and lava flows [9] or for analog modeling of geodynamic processes [10–12], but also in pharmaceutical [13] and food cooking [14] applications. The study of YSMs under thermal convection also takes on a great interest from a fundamental point of view: unlike more standard shear or pressure-driven flows, the forcing is local and dynamic, so the stress configuration across the system is not given *a priori*, but the dynamics itself instead determine it. The non-trivial correlation between such stress configuration and the complex structural fragility landscape can lead to unexpected phenomena in a disordered medium. Experimental [15–19], theoretical and numerical studies [20–26] focused on the onset of convection, looking at the steady-state value of the heat flux (or, conversely, of the temperature difference, in experiments with controlled heat flux) drawing an overall picture whereby yield stress rheology hinders convection. However, the character, the way it is approached, and the very existence of a convective steady-state deserve an in-depth discussion, and this has to be considered an

open problem. Experiments with microgels evidenced how the development of a thermal plume is associated with structural damages in the material, suggesting that plastic microdynamics might play a role. Moreover, unlike in Newtonian convection, the plume can stop and cool down until the emergence of a second plume [15]. Convection arrest following a long period of chaotic oscillations was observed also in numerical simulations [27]. However, a comprehensive study of the long-time behavior of thermal convection in YSMs and the interplay between microscopic constituents and non-linear rheology is still missing. In this Letter, we show that convective heat transfer in a YSM occurs via intermittent heat flux bursts associated with fluidization of the system. The origin of such complex dynamics resides in the elastoplastic character of the material and, therefore, its explanation requires a description that takes into account its granularity (the finite-size droplets microdynamics in the case of emulsions), as suggested also in previous experimental work [19]. In particular, in concentrated emulsions, droplet coalescence eventually leads to a spatially heterogeneous phase inversion, which supports a sustained convection state (see Fig.1(e)).

We perform numerical simulations of a two-dimensional jammed O/W emulsion in the Rayleigh-Bénard setup, i.e., between two parallel no-slip walls at a distance  $H$  with a temperature difference  $\Delta T = T_{\text{hot}} - T_{\text{cold}}$ , subject to the action of gravity (with strength  $g$ ) in the direction of the thermal gradient (see Fig. 1(a)) [28–30]. The Rayleigh number, computed with the transport coefficients of the bulk phase, is  $\text{Ra} = \beta g \Delta T H^3 / (\kappa \nu) \approx 4 \times 10^5$ , where  $\beta$  is the thermal expansion coefficient,  $\kappa$  the thermal diffusivity, and  $\nu$  the kinematic viscosity of the bulk phase, while the Prandtl number  $\text{Pr} = \nu / \kappa$  is fixed to unity. Further details on the employed methodology are reported in the Supplementary Material (SM).

\* f.pelusi@iac.cnr.it

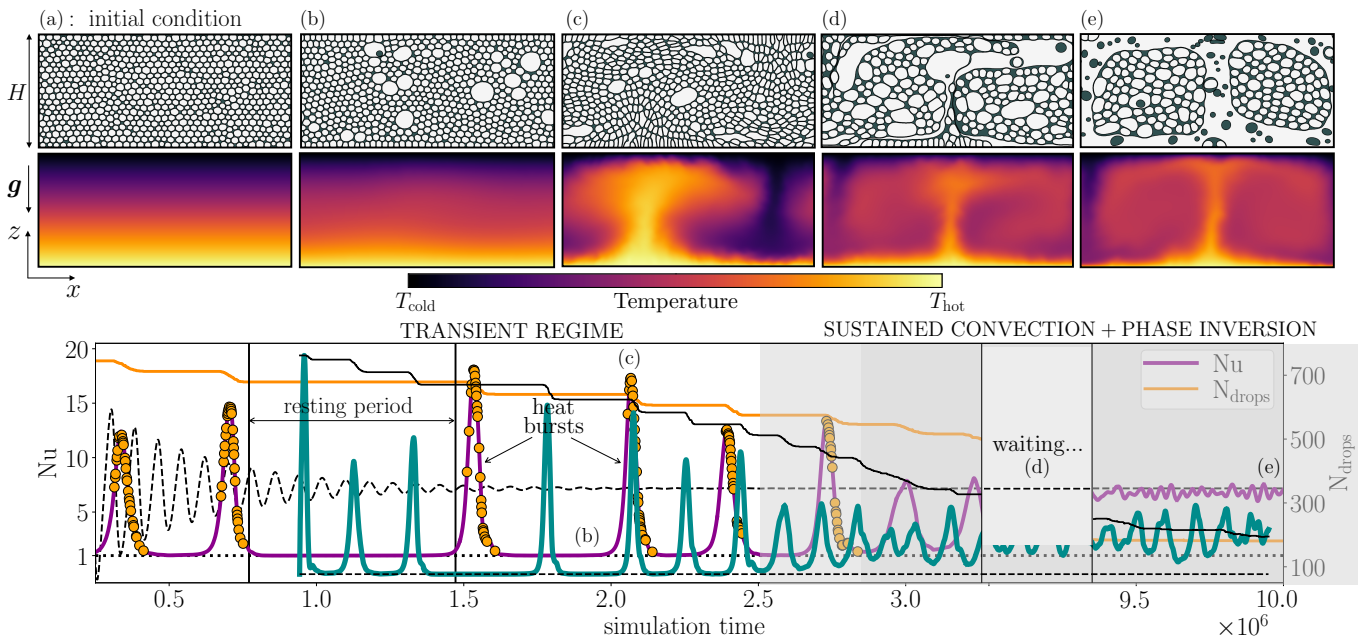


FIG. 1. Dynamics of a concentrated emulsion in a Rayleigh-Bénard convective cell: the time evolution of the average heat transfer is quantified via the Nusselt number  $Nu$ , shown together with the number of droplets  $N_{\text{drops}}$ . A decrease in  $N_{\text{drops}}$  corresponds to the occurrence of coalescence events (an orange bullet ( $\bullet$ ) is drawn any time at least a coalescence event occurs). Dashed black line marks the time evolution of  $Nu$  for a homogeneous system under the same conditions, while dotted line highlights the conductive regime ( $Nu = 1$ ). Upper panels show maps of density (top panels) and temperature fields (lower panels) of selected instants of time ((a)-(e)).

## II. MACROSCOPIC ANALYSIS

After the emulsion preparation (see SM), and the application of a finite perturbation to the hydrodynamical velocity to trigger the thermal convection, we probe the time response of the system by instantaneously measuring the vertical velocity  $u_z = u_z(x, z, t)$  and the temperature  $T = T(x, z, t)$  and computing the dimensionless heat flux expressed by the Nusselt number

$$Nu = 1 + \frac{\langle u_z T \rangle_{x,z}}{\kappa \frac{\Delta T}{H}}, \quad (1)$$

where  $\langle \dots \rangle_{x,z}$  denotes the space average [29–32]. For a single phase (homogeneous) fluid in a purely conductive state, i.e., below the critical value for convection [33], the advective contribution  $\langle u_z T \rangle_{x,z}$  is zero and  $Nu = 1$  (dotted black line in Fig. 1). As  $Ra$  is increased above such a threshold value, the homogeneous fluid reaches a state of steady convection with a large-scale flow, which increases the heat flux in regard to the conduction ( $Nu > 1$ ). Further, for sufficiently large values of  $Ra$ , but ahead of the transition to turbulence, there exist stationary thermal convective states that are stable despite showing oscillations whose amplitude, however, decays exponentially (dashed black line in Fig. 1) [34]. This scenario changes in the case of emulsions, where the value of  $Ra_c$  and the onset to thermal convection depend on the volume fraction  $\phi$  of the dispersed phase. It has been shown in

Refs. [35, 36] that the presence of droplet interactions induces fluctuations in the heat flux (i.e., fluctuations of  $Nu$ ), which increase with  $\phi$ . Following those works, a natural question arises regarding the behavior of emulsions in thermal convection when  $\phi$  is large enough to make the emulsion exhibiting a yield stress: droplets get strongly deformed and endow the emulsion with complex elastic-viscoplastic properties typical of YSMs [3, 37–39]. Hence, we consider jammed emulsions [40] that exhibit a finite yield stress (see SM for a detailed rheological characterization). In Fig. 1, we report the time evolution of  $Nu$  for the emulsion (solid purple line) along with some snapshots of the corresponding density and temperature fields at selected times (panels (a)-(e)). The phenomenology is remarkably different from what observed in Refs. [35, 36] at lower values of  $\phi$ : in the jammed state (i.e., as long as the emulsion can be considered a YSM), the system exhibits a dynamics characterized by extreme heat transfer bursts (convective periods), with  $Nu \gg 1$ , spaced out by long-lasting resting (conductive) periods, with  $Nu \approx 1$ . During the duration of the heat bursts, droplets' coalescence takes place (orange bullets), progressively reducing the number of droplets ( $N_{\text{drops}}$ , orange solid line). Coalescence events decrease the interface energy and eventually lead to the inversion from an O/W to a W/O emulsion, causing the system to persist in a convective state. However, due to the self-organized flow structures (and associated stress configuration), the phase inversion is not global in space but takes place heterogeneously, with

patches of concentrated O/W emulsion around the center of the convective rolls in a matrix of phase-inverted, diluted, W/O emulsions (see Fig. 1(e)). The characterization of the phase-inverted state is particularly intriguing as its rheology diverges significantly from the jammed O/W emulsion (see SM), warranting a dedicated investigation. Here, we focus on the unexpected dynamics in the jammed yield-stress emulsion. In this regime, in correspondence with Nu peaks, the material fluidizes, and convection mixes the temperature field, causing variations of the stress whose amplitude can, locally, go below the yielding point, conferring rigidity again to the material. Surprisingly, after the emulsion stops resting, the motion can restart with a heat transfer burst before the system stops again. The sequence of heat bursts does not display the same regularity of the oscillations in Nu that are observed for the homogeneous system (dashed black line in Fig. 1), and the resulting time needed to achieve the final sustained convective state is much longer than the time it takes for an homogeneous system to reach a stationary convective state. The portrayed scenario is far from being trivial, highlighting that the transition to thermal convection of a highly packed emulsion made up of soft domains shows an anomalous intermittent behavior that profoundly delays the transition to a sustained convective state. Notice that different initial configurations lead to a different duration of the transient intermittent regime and number of heat bursts (see SM, Fig.1). We remark that any attempt to understand this intermittency in terms of continuum equations equipped with a local constitutive relation between stress and shear rate, regularized as the stress tends to the yield value [20, 24, 38, 41], would unavoidably fail. Once the system stops, no mechanism can set it back in motion. Such an approach, indeed, provides misleading information since it is not able to capture the role played by the presence of finite-sized droplets and the change in local microstructure with plastic rearrangements [42], that represent the source of intrinsic effective “noise” able to trigger convection again. Therefore, systematically characterizing the observed scenario would require analysis at scales comparable with the droplet size.

### III. MICROSCOPIC ANALYSIS

Next, we focus on droplets’ microstructure and droplet contribution to heat transfer. In Fig. 2, we report the detection of changes in droplet micro-structures via the analysis of the Delaunay triangulation constructed from the droplets center of mass [43]. Through the Delaunay triangulation, a plastic rearrangement is identified whenever one edge of a droplet shrinks to zero, and neighboring droplets switching occurs (see Fig. 2(a)). In Fig. 2(b), we report the plot of the Nusselt number Nu along with the number of plastic rearrangements  $N_{\text{plastic}}$  in a representative time interval where both heat bursts and resting periods are present. Fig. 2 shows, as ex-

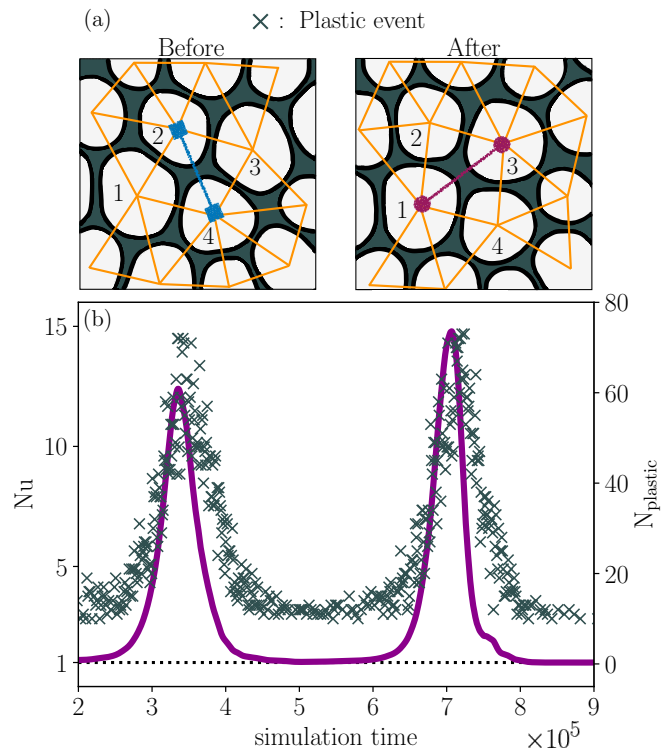


FIG. 2. Panel (a): a sketch describing the definition of plastic event starting from the Delaunay triangulation (orange links). A plastic event takes place when a neighboring droplets switching occurs, corresponding to the disappearance of the link between two droplets (2 and 4) and the creation of a new link between other two (1 and 3). Panel (b): Nusselt number Nu (purple solid line) and the number of occurred plastic events  $N_{\text{plastic}}$  (×) as a function of time.

pected, that  $N_{\text{plastic}}$  grows when the emulsion enters a convective state (heat bursts,  $\text{Nu} \gg 1$ ) but, more interestingly, a residual plastic activity is also apparent during the resting periods, revealing that the macroscopic conductive periods possess non-trivial features at the level of droplets’ microstructure. The latter evidence stimulated further analysis to characterize the heat transfer at the droplet scale. Starting from the  $i$ -th droplet and the associated center-of-mass location  $\mathbf{X}_i(t)$  at a generic time  $t$ , we considered the velocity,  $u_z^{(i)} = u_z(\mathbf{X}_i(t))$ , temperature,  $T^{(i)} = T(\mathbf{X}_i(t))$ , and temperature gradient,  $(\partial_z T)^{(i)} = \partial_z T(\mathbf{X}_i(t))$ , and we defined the Nusselt number at the droplet scale  $\text{Nu}_i^{(\text{drop})}$  [35, 36]

$$\text{Nu}_i^{(\text{drop})} = \frac{u_z^{(i)} T^{(i)} - \kappa (\partial_z T)^{(i)}}{\kappa \frac{\Delta T}{H}}. \quad (2)$$

This definition is such that the macroscopic Nusselt number Nu (Eq. 1) can be reconstructed as the sum over the contributions of each single droplet,  $\text{Nu} \approx \frac{1}{N_{\text{drops}}} \sum_{i=1}^{N_{\text{drops}}} \text{Nu}_i^{(\text{drop})}$  (see SM, Fig. 3). Via the analysis of  $\text{Nu}_i^{(\text{drop})}$ , we can shed light on the microscopic origin of the intermittency in Nu at macroscales. Fig. 3 shows the

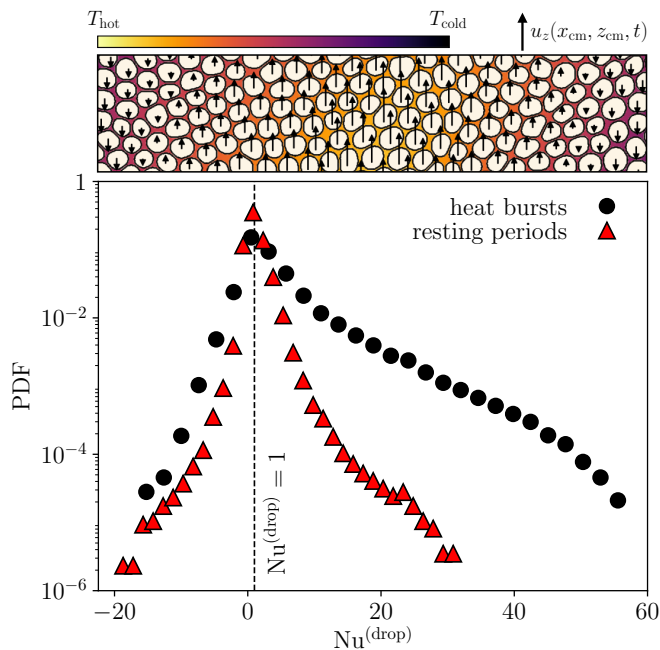


FIG. 3. Probability distribution functions (PDFs) of the Nusselt number at the droplet scale  $Nu^{(\text{drop})}$  (see Eq. (2)), for droplets contributing to heat bursts (●) and resting periods (▲). Upper panel: temperature map along with the droplets' center-of-mass, with the corresponding vertical velocity vectors used to compute  $Nu^{(\text{drop})}$ .

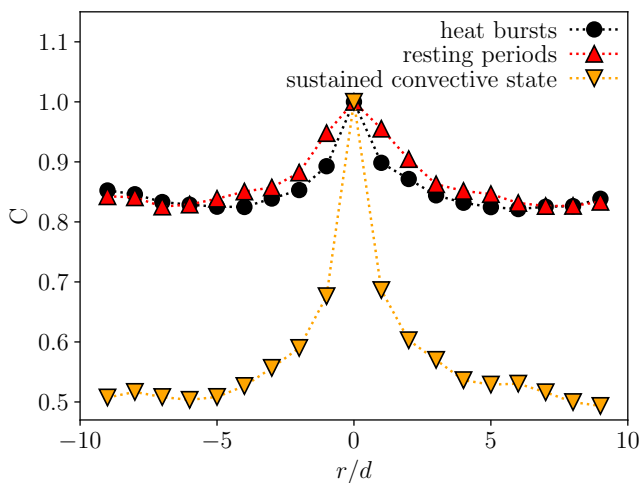


FIG. 4. Correlation function  $C$  of interface displacement (see Eq. (3)) as a function of the distance from the center of the channel  $r$  normalized with the average droplet diameter  $d$ . We compare correlation functions for heat bursts (●) and resting periods (▲). Correlation function computed during the sustained convective state after the transient dynamics is also shown (▼).

probability distribution function (PDF) for  $Nu^{(\text{drop})}$  during the transient intermittent dynamics, where we separately examined the contributions to heat bursts periods and the resting periods. Specifically, we collected the val-

ues of  $Nu_i^{(\text{drop})}$  associated with every droplet at any time during the two periods mentioned above and, to improve the statistics, we considered tens of numerical simulations for different initial configurations. The resulting statistics of  $Nu^{(\text{drop})}$  reveals enhanced tails and clear intermittency during the heat bursts. As a matter of fact, the average value of the distribution is sensibly larger than the most probable value; additionally, when the system is at rest, the statistics of  $Nu^{(\text{drop})}$  features a non-zero variance, indicating that heat is transferred at the scales of the droplets. However, on average, the system at the macroscopic scale is in a conductive state ( $Nu \approx 1$ ). The presence of residual elastoplastic activity shown both in Fig. 2 and in Fig. 3 is inherently related to the presence of finite-size droplets and acts as a perturbation on the system during the macroscopic resting periods when  $Nu \approx 1$ . A natural question arises on the mechanism that allows the system to move from the resting periods to the heat bursts. The effect of localized perturbations can be spread over the system size if its spatio-temporal correlation is sufficiently large [44]. The presence of residual plastic activity due to spatial heterogeneity may catalyze the observed irregularity and intermittency in heat transfer bursts. A confirmation of the system's extensive spatial correlation is, therefore, essential. To define a quantitative measure of the correlations associated with the motion of the interface during and after the transient dynamics (i.e., when it becomes difficult to identify and follow each droplet), we follow the procedure introduced in Ref. [45]: we divide the domain into squares with a side of length  $d$  (average droplet diameter), then for each square  $k$  we consider two consecutive times  $t$  and  $t + \tau$ . We compute the interface displacement as  $A^{(\tau)}(x_k, z_k, t) = \langle [\rho_O(x, z, t + \tau) - \rho_O(x, z, t)]^2 \rangle_k$ , where  $\rho_O$  is the density field of the "oil" phase and  $\langle \dots \rangle_k$  denotes the average in square  $k$  with center coordinates  $(x_k, z_k)$ . Then, we compute the correlation function  $C$  of  $A_r^{(\tau)} = A^{(\tau)}(x_k, r, t)$  as

$$C = \left\langle \frac{\langle A_0^{(\tau)} A_r^{(\tau)} \rangle_t - \langle A_0^{(\tau)} \rangle_t \langle A_r^{(\tau)} \rangle_t}{\sigma_0 \sigma_r} \right\rangle_x, \quad (3)$$

where  $r$  denotes the distance from the channel center ( $z_k = 0$ ) along the  $z$ -direction,  $\langle \dots \rangle_t$  is the average over times belonging to the three different regimes (see SM), and  $\sigma_r$  is the standard deviation of  $A_r^{(\tau)}$ .  $C$  is reported in Fig. 4. It emerges that, during heat bursts, the thermal plume dynamically engages nearly the entire system, resulting in a notable correlation. Surprisingly, this correlation remains large even during resting periods, which is unexpected in a homogeneous system in conductive state, where the absence of fluid motion typically implies no motion, hence the lack of any correlation. Notably, when the system sustains a convective state and initiates phase inversion, the correlation decreases, evidencing the absence of intermittent behavior.

#### IV. CONCLUSIONS

We studied the long-time behavior of a typical YSM, i.e., a jammed emulsion, under thermal convection. We pointed out a novel phenomenon, never reported before, whereby convection occurs through fluidization-rigidity transitions, entailing heat flux bursts occurring in an otherwise conductive background. Once thermal convection is initiated, temperature field mixing causes stress fluctuations leading to a halting of convection if the stress drops below the yield value. Leveraging on numerical simulations [46], we can observe that, remarkably, residual plastic activity persists even during macroscopic resting periods, thus acting as a latent trigger for subsequent convective events. This plasticity stems from the inherently disordered structure of the emulsion, resulting in an intermittent onset of convective transport without discernible regularity, which cannot be predicted based on continuum equations coupled with bulk rheology. Fluidization events and heat bursts are associated with droplets' coalescence, eventually leading to a phase-inverted emulsion exhibiting spatial heterogeneity: to our knowledge, such a final state remains unexplored and warrants fur-

ther investigation, both morphologically and rheologically. For a given emulsion, we studied the intermittency phenomenon at a fixed Rayleigh number (Ra), and we expect that it can only survive in a specific range of Ra. Indeed, for very low Ra values, convection is suppressed, whereas for large Ra values a quicker transition to the convective state in the phase-inverted emulsion is prompted through more frequent coalescence events, bypassing the intermittent behavior.

Altogether, we argue that our findings open new fundamental views on the transition to sustained convection in jammed emulsions, which occurs through a rather unusual transient and intermittent behavior and leads to heterogeneous phase inversion.

#### ACKNOWLEDGEMENTS

This work has been carried out within the TEX-TAROSSA project (G.A. H2020-JTI-EuroHPC-2019-1 No. 956831). MS and MB acknowledge the support of the National Center for HPC, Big Data and Quantum Computing, Project CN\_00000013 - CUP E83C22003230001, Mission 4 Component 2 Investment 1.4, funded by the European Union - NextGenerationEU.

- 
- [1] R. G. Larson, *The Structure and Rheology of Complex Fluids* (Oxford University Press, 1999).
  - [2] P. Coussot, *Rheometry of Pastes, Suspensions, and Granular Materials* (Wiley-Interscience, 2005).
  - [3] D. Bonn, M. M. Denn, L. Berthier, T. Divoux, and S. Manneville, *Reviews of Modern Physics* **89**, 035005 (2017).
  - [4] E. Orowan, *Philosophical Transactions of the Royal Society A* **258**, 284 (1965).
  - [5] W. J. Morgan, *Nature* **230**, 42 (1971).
  - [6] R. Montelli, G. Nolet, F. Dahlen, and G. Masters, *Geochemistry, Geophysics, Geosystems* **7** (2006).
  - [7] S. French and B. Romanowicz, *Nature* **525**, 95 (2015).
  - [8] A. Davaille, P. Carrez, and P. Cordier, *Geophysical Research Letters* **45**, 1349 (2018).
  - [9] R. Griffiths, *Annual Review of Fluid Mechanics* **32**, 477 (2000).
  - [10] W. Schellart and V. Strak, *Journal of Geodynamics* **100**, 7 (2016).
  - [11] E. Di Giuseppe, F. Corbi, F. Funicello, A. Massmeyer, T. Santimano, M. Rosenau, and A. Davaille, *Tectonophysics* **642**, 29 (2014).
  - [12] J. Reber, M. Cooke, and T. Dooley, *Earth-Science Reviews* **202**, 103107 (2020).
  - [13] G. Marti-Mestres and F. Nielloud, *Journal of Dispersion Science and Technology* **23**, 419 (2002).
  - [14] H. Jeffreys, *St. John's Coll. Camb. Sir Harold Jeffreys Pap.* **C17** (1957).
  - [15] A. Davaille, B. Gueslin, A. Massmeyer, and E. Di Giuseppe, *Journal of Non-Newtonian Fluid Mechanics* **193**, 144 (2013).
  - [16] M. Darbouli, C. Métivier, J.-M. Piau, A. Magnin, and A. Abdelali, *Physics of Fluids* **25**, 023101 (2013).
  - [17] Z. Kebiche, C. Castelain, and T. Burghelea, *Journal of Non-Newtonian Fluid Mechanics* **203**, 9 (2014).
  - [18] C. Metivier, C. Li, and A. Magnin, *Physics of Fluids* **29**, 104102 (2017).
  - [19] K. Jadhav, P. Rossi, and I. Karimfazli, *Journal of Fluid Mechanics* **912**, A10 (2021).
  - [20] O. Turan, N. Chakraborty, and R. J. Poole, *Journal of Non-Newtonian Fluid Mechanics* **171-172**, 83 (2012).
  - [21] I. Karimfazli, I. Frigaard, and A. Wachs, *Journal of Fluid Mechanics* **787**, 474 (2016).
  - [22] C. Li, A. Magnin, and C. Métivier, *AIChE Journal* **62**, 1347 (2016).
  - [23] M. S. Aghighi, A. Ammar, C. Metivier, and M. Gharagozlu, *International Journal of Thermal Sciences* **127**, 79 (2018).
  - [24] H. Masoumi, M. Aghighi, A. Ammar, and A. Nourbakhsh, *International Journal of Heat and Mass Transfer* **138**, 1188 (2006).
  - [25] P. R. Santos, A. Lugarini, S. L. Junqueira, and A. T. Franco, *International Journal of Thermal Sciences* **166**, 106991 (2021).
  - [26] M. S. Aghighi, C. Metivier, and S. Fakhri, *Multidiscipline Modeling in Materials and Structures* **19**, 1275 (2023).
  - [27] A. Vikhansky, *Physics of Fluids* **21** (2009).
  - [28] S. Grossmann and D. Lohse, *Physical Review Letters* **86**, 3316 (2001).
  - [29] G. Ahlers, S. Grossmann, and D. Lohse, *Reviews of Modern Physics* **81**, 503 (2009).
  - [30] F. Chillà and J. Schumacher, *The European Physical Journal E* **35**, 1 (2012).

- [31] B. I. Shraiman and E. D. Siggia, *Physical Review A* **42**, 3650 (1990).
- [32] R. J. Stevens, R. Verzicco, and D. Lohse, *Journal of Fluid Mechanics* **643**, 495 (2010).
- [33] S. Chandrasekhar, *Hydrodynamic and hydromagnetic stability* (Oxford University Press, 1961).
- [34] R. Ecke, H. Haucke, Y. Maeno, and J. Wheatley, *Physical Review A* **33**, 1870 (1986).
- [35] F. Pelusi, M. Sbragaglia, R. Benzi, A. Scagliarini, M. Bernaschi, and S. Succi, *Soft Matter* **17**, 3709 (2021).
- [36] F. Pelusi, S. Ascione, M. Sbragaglia, and M. Bernaschi, *Soft Matter* **19**, 7192 (2023).
- [37] H. Princen and A. Kiss, *J. Colloid Interface Sci.* **128**, 176 (1989).
- [38] J. Zhang, D. Vola, and I. A. Frigaard, *Journal of Fluid Mechanics* **566**, 389 (2006).
- [39] N. J. Balmforth, I. A. Frigaard, and G. Ovarlez, *Annual Review of Fluid Mechanics* **46**, 121 (2014).
- [40] The nominal volume fraction is  $\phi = 80\%$ , corresponding to an effective volume fraction  $\phi_{\text{eff}} \approx \phi(1 + 2h/d) \approx 93\%$ , corrected as in [T. Mason, J. Bibette, and D. Weitz, *Physical Review Letters* **71**, 2051 (1995).] to account for the film thickness  $h$ .
- [41] N. J. Balmforth and A. C. Rust, *Journal of Non-Newtonian Fluid Mechanics* **158**, 36 (2009).
- [42] J. Goyon, A. Colin, G. Ovarlez, A. Ajdari, and L. Bocquet, *Nature* **454**, 84 (2008).
- [43] M. Bernaschi, M. Lulli, and M. Sbragaglia, *Computer Physics Communications* **213**, 19 (2017).
- [44] F. Pelusi, M. Sbragaglia, and R. Benzi, *Soft Matter* **15**, 4518 (2019).
- [45] R. Benzi, P. Kumar, F. Toschi, and J. Trampert, *Geophysical Journal International* **207**, 1667 (2016).
- [46] F. Pelusi, M. Lulli, M. Sbragaglia, and M. Bernaschi, *Computer Physics Communications* **273**, 108259 (2022).